

# TOWARDS REALISTIC INCREMENTAL SCENARIO IN CLASS INCREMENTAL SEMANTIC SEGMENTATION

**Jihwan Kwak**

Seoul National University  
{kkwakzi}@snu.ac.kr

**Sungmin Cha**

New York University  
{sungmin.cha}@nyu.edu

**Taesup Moon**

Seoul National University  
{tsmoon}@snu.ac.kr

## ABSTRACT

This paper addresses the unrealistic aspect of the commonly adopted Continuous Incremental Semantic Segmentation (CISS) scenario, termed *overlapped*. We point out that *overlapped* allows the **same** image to reappear in future tasks with different pixel labels, which is far from practical incremental learning scenarios. Moreover, we identified that this flawed scenario may lead to biased results for two commonly used techniques in CISS, pseudo-labeling and exemplar memory, resulting in unintended advantages or disadvantages for certain techniques. To mitigate this, a practical scenario called *partitioned* is proposed, in which the dataset is first divided into distinct subsets representing each class, and then the subsets are assigned to each corresponding task. This efficiently addresses the issue above while meeting the requirement of CISS scenario, such as capturing the background shifts. Furthermore, we identify and address the code implementation issues related to retrieving data from the exemplar memory, which was ignored in previous works. Lastly, we introduce a simple yet competitive memory-based baseline, MiB-AugM, that handles background shifts of current tasks in the exemplar memory. This baseline achieves state-of-the-art results across multiple tasks involving learning numerous new classes.

## 1 INTRODUCTION

Due to increasing industrial demands, recent studies have placed significant emphasis on understanding the behavior of models when learning from non-stationary streams of data. One area of particular interest is the Class Incremental Learning (CIL) problem, where a model learns new classes from incrementally arriving training data. The primary challenge in CIL lies in addressing the plasticity-stability dilemma (Carpenter & Grossberg, 1987; Mermillod et al., 2013), whereby models must learn new concepts while mitigating the risk of *catastrophic forgetting* (McCloskey & Cohen, 1989), a phenomenon of inadvertently forgetting previously acquired knowledge when learning new concepts. To date, research in this field has expanded beyond methodological approaches (Kirkpatrick et al., 2017; Lopez-Paz & Ranzato, 2017; Yoon et al., 2017) to include discussions on practical scenarios (Wu et al., 2019; Tao et al., 2020; He et al., 2020) that closely mirror real-world learning processes.

Motivated by its applications to autonomous driving and robotics, CIL has extended its reach to semantic segmentation tasks, known as Class Incremental Semantic Segmentation (CISS). In CISS, the model additionally encounters the challenge of *background shift* (Cermelli et al., 2020), which refers to a semantic drift of the background class between tasks. Specifically, since all pixels whose ground truth class does not correspond to the current task classes are annotated as background, objects from previous and future classes may be mislabeled as background. This exacerbates the forgetting of previous classes and hinders the knowledge acquisition of new classes.

To apply and evaluate CISS methods, two incremental scenarios, *disjoint* and *overlapped* were initially introduced by Cermelli et al. (2020). Since the *disjoint* scenario failed to capture the background shift of unseen classes, most studies (Douillard et al., 2021; Baek et al., 2022; Zhang et al., 2022a; 2023) have focused on *overlapped*. Notably, recent methods have demonstrated state-of-the-art performance by either freezing parameters (Cha et al., 2021; Zhang et al., 2022b) or applying strong regularization (Baek et al., 2022; Zhang et al., 2023). However, despite the active discussion on methodologies, there is a lack of awareness about the limitations of the *overlapped* scenario, which have been overlooked until now.

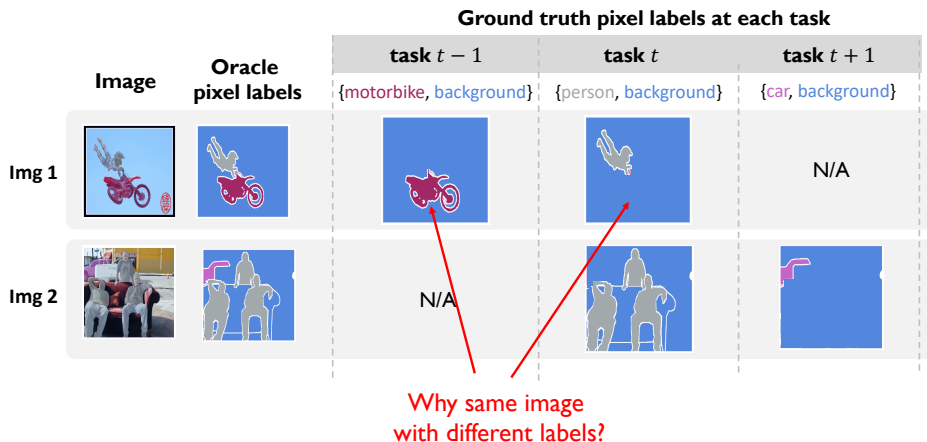


Figure 1: A figure that depicts the incremental scenario and labeling rule of *overlapped*. It shows how the pixel labels of each image is given at each task. Notably, the same image is given in future tasks with a pixel labels that does not contain information about previous task labels.

In this work, our focus lies on addressing the issue of the unrealistic aspect present in the commonly adopted scenario of CISS, termed *overlapped*. As depicted in Figure 1, in the overlapped scenario, the **same image** can be reintroduced in future tasks with **different** pixel labels. For instance, an image of a man with a motorbike may appear in both task  $t - 1$  and task  $t$  with distinct pixel labels: one with motorbike annotation and the other with person.

To strengthen our argument, we emphasize that this flawed setting can lead to unwanted advantages or disadvantages to certain techniques, consequently affecting the development and adoption of algorithms in real-world applications. We confirmed that overlapping data can result in several issues with commonly used methods in CISS:

- Pseudo-labeling on previously seen overlapping data using a previously learned model may confer unfair advantages in retrieving past class labels.
- Overlapping data saved in exemplar memory may cause a label conflict when the same image is reintroduced in a new task with different pixel labels.

As an alternative, we propose a practical scenario, dubbed as *partitioned*, that facilitates accurate and objective evaluation of CISS algorithms. This involves partitioning the dataset into mutually distinct subsets, each representing a specific class, and assigning each subset to its corresponding task. This methodology effectively eliminates unnecessary artifact of *overlapped* while satisfying the preconditions of CISS scenario, such as capturing the background shifts of both previous and unseen classes.

Furthermore, we address the overlooked code implementation issues in memory retrieval, which is ignored in prior studies. Prior code frameworks rather provide labels of the current task to the retrieved data.

Lastly, motivated by the issues above, we introduce an efficient memory-based baseline, named MiB-AugM, that effectively handles the background shift of the current task class in the exemplar memory. Experiments with reproduced baselines show that our method outperforms state-of-the-art methods across several tasks involving the learning of numerous new classes at every task.

## 2 RELATED WORKS

### 2.1 CLASS INCREMENTAL LEARNING (CIL)

**Methodologies** Research on CIL has primarily focused on image classification tasks, with methods falling into three main categories: 1) *Regularization*-based (Kirkpatrick et al., 2017; Chaudhry et al., 2018; Ahn et al., 2019; Jung et al., 2020), 2) *Rehearsal*-based (Lopez-Paz & Ranzato, 2017; Shin et al., 2017; Prabhu et al., 2020), and 3) *Architecture*-based (Rusu et al., 2016; Yoon et al., 2017; Hung et al., 2019; Yan et al., 2021a) solutions. Among them, approaches that combine *regularization* through knowledge distillation (KD) (Hinton et al., 2015) and *rehearsal* of exemplar memory (Rolnick et al., 2019) have achieved state-of-the-art performance (Li & Hoiem, 2017; Buzzega et al., 2020).

Consequently, this integration has spurred a line of research dedicated to addressing by-product problems such as prediction bias (Wu et al., 2019; Ahn et al., 2021).

**Incremental scenarios** Since the research demands of continual learning started from the non-stationary property of the real-world, several works have claimed the necessity of building up a practical incremental scenario that resembles the learning process of the real-world. For example, Wu et al. (2019); Ahn et al. (2021) suggested an evaluation on *large scale* CIL scenarios and Hou et al. (2019); Douillard et al. (2020) proposed a scenario that includes a *large base task* where the model has a chance to initially learn knowledge from many classes.

With growing concerns about realistic scenarios that align with industrial demands, CIL studies have stretched out its application to settings with additional data constraints such as *few-shot* (Tao et al., 2020; Yang et al., 2023) or *online* (He et al., 2020; Lin et al., 2023). Similarly, a new body of discussions on *online*-CIL regarding practical scenarios (Koh et al., 2022; Chrysakis & Moens, 2023) or constraints (Ghunaim et al., 2023) has been introduced.

## 2.2 CLASS INCREMENTAL SEMANTIC SEGMENTATION (CISS)

**Methodologies** Inspired by recent works of CIL, initial works in CISS (Cermelli et al., 2020; Douillard et al., 2021; Michieli & Zanuttigh, 2021) took KD-based regularization as a general approach. MiB (Cermelli et al., 2020) proposed a novel KD-based regularization to address the semantic drift of background label. PLOP (Douillard et al., 2021) brought the idea of Douillard et al. (2020) and utilized the feature-wise KD. On the other hand, few works (Yan et al., 2021b; Zhu et al., 2023) focused on employing the exemplar memory. Yan et al. (2021b) proposed to use a class-balanced memory but only focused on *online* setting. Zhu et al. (2023) proposed a memory sampling mechanism to ensure diversity among samples but has a reproduction issue<sup>1</sup>. Recently, SSUL (Cha et al., 2021) which introduced a method to freeze the feature extractor have demonstrated outperforming performance. As a result, the recent state-of-the-art CISS methods have been focused on either freezing (Zhang et al., 2022b) or regularizing the extractor with hard constraint (Zhang et al., 2023; Chen et al., 2023), while considering memory usage as an extra factor to enhance performance slightly.

**Incremental scenarios** Cermelli et al. (2020) first established the learning scenarios of CISS, *overlapped* and *disjoint* on Pascal VOC 2012 (Everingham et al., 2010) and ADE 20K (Zhou et al., 2017). After many works (Douillard et al., 2021; Baek et al., 2022) pointed out the impractical assumption of *disjoint* where the existence of semantic shift of unseen class is excluded, current CISS research is actively being explored in *overlapped* scenario. However, in contrast to CIL, where both practical scenarios and methodologies have been actively discussed, there has been no further discussion on the learning scenarios in CISS until now.

Building upon insights acquired from previous studies of CIL in classification, regularization-based methods have achieved impressive performance in CISS. However, previous studies have often overlooked the practical considerations in the learning scenarios. In this work, we point out an overlooked issue in the learning scenario (e.g., overlapped) and propose a new scenario and a competitive baseline method that effectively leverages the exemplar memory.

## 3 PROPOSED SCENARIO AND REPLAY-BASED BASELINE

### 3.1 NOTATION AND PROBLEM SETTING

Class Incremental Learning (CIL) for image classification operates under the assumption that pairs of input data and its corresponding label for *new* classes are accessible for training a model in each incremental *task*. At each task  $t$ , the model is trained on a new dataset,  $\mathcal{D}^t$  annotated with a set of new classes  $\mathcal{C}^t$ . In the evaluation phase, the model is expected to distinguish between all the seen classes up to task  $t$ , denoted as  $\mathcal{C}^{0:t} = \mathcal{C}^0 \cup \dots \cup \mathcal{C}^t$ . Each task is organized with disjoint classes, meaning there is no overlap of classes between the tasks, denoted as  $\mathcal{C}^i \cap \mathcal{C}^j = \emptyset$  for  $\forall i, j$ . Note that the model initially acquires knowledge of a large number of classes at the base task (task 0), and gradually learns the remaining classes in subsequent tasks (task 1 to  $T$ ).

Class Incremental Semantic Segmentation (CISS) considers incremental learning in semantic segmentation, involving the pixel-level prediction of labels. At task  $t$ , an input image  $x \in \mathbb{R}^{H \times W \times 3}$  is paired with its corresponding pixel labels  $y \in \mathbb{R}^{H \times W}$ , denoted as  $(x, y) \sim \mathcal{D}^t$ . Each mask  $y$  includes at least one pixel annotated as one of the classes in  $\mathcal{C}^t$ , i.e.,  $\exists i \in \mathcal{I} s.t. y_i \in \mathcal{C}^t$ , where  $\mathcal{I}$  indicates the set of indexes of pixels in an image. Pixels not belonging to  $\mathcal{C}^t$  are labeled as the background label  $c_{bg}$ . Therefore, each task dataset  $\mathcal{D}^t$  in CISS contains ground truth labels corresponding to  $\mathcal{C}^t \cup c_{bg}$ . Note that objects from the *past* or *future* task’s classes may be labeled as the background label in the current dataset  $\mathcal{D}^t$ , even though these same objects have their actual labels in other tasks. This label shift

<sup>1</sup>The code for the implementation is not available

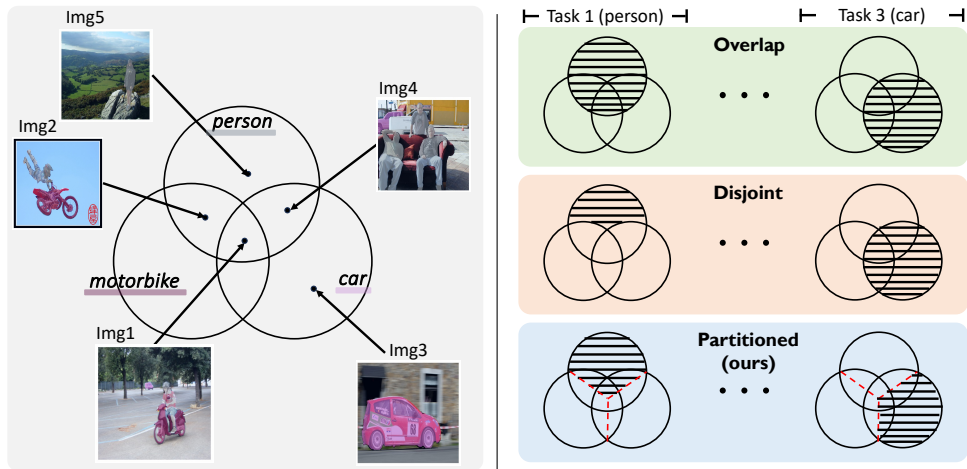


Figure 2: **(Left)** A Venn diagram illustrating the relationship between ground truth class for each datum. Each datum is assigned to a class set based on the object it contains. **(Right)** Comparison of  $\mathcal{D}^t$  (highlighted with black line) for each scenario. Table 4 in the Appendix provides a detailed summary of the assigned labels for each image in every incremental task.

between tasks, known as *background shift*, presents a significant challenge in CISS. Previous works have considered two scenarios of CISS, *overlapped* and *disjoint*, which will be discussed in Section 3.2. Following previous works (Cha et al., 2021; Baek et al., 2022), we also introduce an exemplar memory  $\mathcal{M}^{t-1}$ , which stores a subset of data from  $\mathcal{D}^{0:t-1}$  and is used for task  $t$ . The size of memory remains consistent across the tasks, denoted as  $|\mathcal{M}^t| = M \forall t$ .

At task  $t$ , our model, parameterized by  $\theta^t$ , consists of a feature extractor and a classifier, denoted as  $f_{\theta^t}(\cdot)$ . Given an input  $x$ , the model produces a consolidated score of seen classes for each pixel  $z_i^t = f_{\theta^t}(x)_i \in \mathbb{R}^{|\mathcal{C}^{0:t} \cup \{c_{bg}\}|}$ . The class prediction for each pixel is obtained by selecting the class with the highest score:

$$\hat{y}_i^t = \arg \max_{c \in \mathcal{C}^{0:t} \cup \{c_{bg}\}} z_{i,c}^t, \quad (1)$$

where  $z_{i,c}^t$  represents the output score (before softmax) of the model for a class  $c$ .

### 3.2 INCREMENTAL SCENARIOS IN CISS: DISJOINT AND OVERLAPPED

Two incremental scenarios have been recognized as key scenarios of CISS (Cermelli et al., 2020): *overlapped* and *disjoint*. The dataset construction of each scenario can be compared using a set diagram, as depicted in Figure 2.

Suppose we are constructing a CISS scenario using a dataset that has three object classes (*motorbike*, *car*, and *person*), as annotated in Figure 2. First, we can define three sets representing each class, in which the element in a set represents a datum (*i.e.*, a pair of  $(x, y)$ ). Each datum is then assigned to one or more class sets based on the labels of its *oracle* pixel labels. For example, the figure illustrates that *Img1* and *Img2* have objects whose pixels are labeled as  $\{car, motorbike, person\}$  and  $\{motorbike, person\}$ , respectively. In this case, both *Img1* and *Img2* are elements of *motorbike* class set. Then, as illustrated in Figure 2 (right), we can use the Venn diagram of three sets to demonstrate the dataset given at each task in CISS. Namely, the data points covered by black lines indicate the dataset utilized for each task.

As illustrated in the right figure, *disjoint* ensures the separation of the dataset for each task but necessitates prior knowledge of unseen classes to achieve this separation (Cermelli et al., 2020). Moreover, *disjoint* does not capture the background shift of classes from future tasks, leading to the widespread adoption of the *overlapped* scenario in recent works (Cermelli et al., 2020; Douillard et al., 2020; Cha et al., 2021). However, we argue that the *overlapped* scenario has its own set of challenges.

### 3.3 UNREALISTIC PROPERTIES OF THE OVERLAPPED SCENARIO

The problem arises from the fact that, in *overlapped*, previously seen images may be reintroduced in future tasks with different pixel labels, as illustrated in Figure 1. For example, in Figure 1, the pixel labels of *Img1* in task  $t - 1$  contain

labels of pixels corresponding to the motorbike object, while all other pixels are annotated as the *background* class. However, in task  $t$ , the **same** image is labeled only with the *person* class, leaving the remaining pixels, including the motorbike object, as the *background* class. In this work, we term this problematic data as *overlapping data*, and argue that this overlapping data is the root cause of the overlapped scenario being far from a practical incremental learning scenario.

This impractical setting in CISS may pose a significant problem, as experiments conducted in these settings can lead to misleading conclusions, potentially impacting the development and adoption of algorithms in practical applications. In this section, we provide examples and evidence demonstrating that these unrealistic aspects, *i.e.*, overlapping data, can lead to biased results for certain methods commonly used in CISS.

**Unwanted advantages of pseudo-labeling with previously learned model** Pseudo-labeling with a previously learned model facilitates the retrieval of previous class labels if it is worked on already seen overlapping data, which can provide unnecessary advantages. To mitigate the issues arising from background shift caused by classes from the previous task, many recent studies (Douillard et al., 2021; Cha et al., 2021; Zhang et al., 2023; Chen et al., 2023) employ pseudo-labeling for the background region using predictions from the previously learned model. Formally, the pseudo-label  $\tilde{y}_i$  can be defined as follows:<sup>2</sup>

$$\tilde{y}_i = \begin{cases} y_i & \text{if } y_i \in \mathcal{C}^t \\ \hat{y}_i^{t-1} & \text{if } (y_i = c_{bg}) \wedge (s_i^{t-1} > \tau) \\ c_{bg} & \text{otherwise,} \end{cases} \quad (2)$$

where  $s_i^{t-1} = \max_{c \in \mathcal{C}^{0:t-1} \cup \{c_{bg}\}} \frac{z_{i,c}^{t-1}}{\sum_k z_{i,k}^{t-1}}$  represents the confidence of the prediction (after softmax) for  $\hat{y}_i^{t-1} \in \mathcal{C}^{0:t-1} \cup \{c_{bg}\}$  and  $\tau$  indicates the confidence threshold for pseudo-labeling, respectively. An issue arises when the model revisits the **same** training images. Since the model previously learned certain objects that are now labeled as background, it is likely to yield high prediction scores for those objects and, as a result, to restore most of its labels. Consequently, these overlapping images contribute to an increased retrieval of past class labels through pseudo-labeling.

To showcase the aforementioned phenomenon, we conducted experiments with the Pseudo-labeling Retrieval Rate (PRR) metric, defined as follows:

$$PRR(y_{oracle}, \tilde{y}^{t-1}) = \frac{1}{|\hat{D}|} \sum_{(x, y_{oracle}) \sim \hat{D}} \text{mIoU}_{\mathcal{C}^{0:t-1} \cup \{c_{bg}\}}(y_{oracle}, \tilde{y}^{t-1}) \quad (3)$$

where  $\hat{D}$  indicates the dataset under evaluation that includes image  $x$  with  $y_{oracle}$  which indicates an oracle pixel labels containing all foreground and background classes. Also,  $\tilde{y}^{t-1}$  denotes the pseudo-label of  $x$  generated by  $f_{\theta^{t-1}}$ . To assess the retrieval rate of previous classes, Intersection-over-Unions (IoU) between  $\tilde{y}^{t-1}$  and  $y_{oracle}$  is averaged among previous classes, denoted as  $\text{mIoU}_{\mathcal{C}^{0:t-1} \cup \{c_{bg}\}}(\cdot, \cdot)$ . For an in-depth understanding of the PRR metric, please refer to the Figure 6.

For verification, we modify the overlapped scenario by randomly dividing the overlapping data of two consecutive tasks into two parts with the same size. One part will be seen at the previous task, task  $t-1$ , denoted by  $\mathcal{D}_{seen}^t$ , and the other will not be seen, denoted by  $\mathcal{D}_{unseen}^t$ . So, at task  $t-1$ , the model is trained with  $\mathcal{D}_{seen}^t$  and non-overlapping data of  $\mathcal{D}^{t-1}$ . After training the model  $f_{\theta^{t-1}}$ , we evaluate the PRR results of  $\mathcal{D}_{seen}^t$  and  $\mathcal{D}_{unseen}^t$  by comparing IoU between oracle labels and pseudo-labels generated from  $f_{\theta^{t-1}}$ .

Table 1 demonstrates PRR results of CISS baselines across different task settings, task 15-1 and task 15-5. Experiments are done on PASCAL VOC 2012 (Everingham et al., 2010) and task 15-1 indicates that the model initially learns 15 classes and incrementally learns 1 class at every task. Since the evaluation is done on task 1, PRR is evaluated after learning 15 classes, task 0. For baselines, we use two common methods in CISS, MiB (Cermelli et al., 2020) and DKD (Baek et al., 2022). Detailed configuration of each dataset and IoU results of each class are written the appendix.

Table 1: Pseudo-labeling Retrieval Rate (PRR) between the oracle label and the pseudo-label generated by a previously learned model of each method. The evaluation is done at task 1.

	15-1 Task ( $t=1$ )		15-5 Task ( $t=1$ )	
	$\mathcal{D}_{seen}^t$	$\mathcal{D}_{unseen}^t$	$\mathcal{D}_{seen}^t$	$\mathcal{D}_{unseen}^t$
MiB (Cermelli et al., 2020)	79.60	64.85 (14.75 ↓)	85.94	61.11 (24.83 ↓)
DKD (Baek et al., 2022)	78.58	65.86 (12.72 ↓)	84.92	59.00 (25.92 ↓)

<sup>2</sup>Since each study follows different rules for pseudo-labeling, we present the simplest format. Note that the core idea of pseudo-labeling is to use the predicted labels with a high prediction score, which is steered by hyper-parameter  $\tau$ .

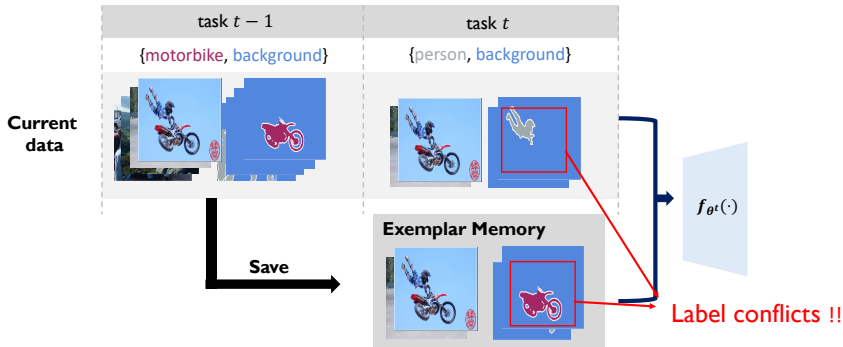


Figure 3: Illustration of a label conflict caused by overlapping data. Note that the pixel labels of an identical image are inconsistent, pixel labels at task  $t$  being annotated with person class and pixel labels from exemplar memory annotated with motorbike class.

Compared to PRR results of  $\mathcal{D}_{seen}^t$ , PRR results of  $\mathcal{D}_{unseen}^t$  shows a notable decline in both 15-1 and 15-5 tasks. Particularly in the 15-5 task, where the size of the overlapping data gets bigger, both baselines show a larger decrease, 24.83 and 25.92 respectively.

These experimental findings illustrate that the retrieval of previous labels in overlapping data is relatively straightforward and, as a result, pseudo-labeling techniques take advantage of the unrealistic aspect of overlapped, *i.e.*, overlapping data, which may result in biased comparison in CISS.

**Unwanted disadvantages of using exemplar memory** If the overlapping data is saved and replayed in future tasks, it can cause *label conflict* between the **same** image that has a different pixel labels. Recent studies (Cha et al., 2021; Baek et al., 2022; Zhu et al., 2023; Chen et al., 2023) also actively utilize exemplar memory to store and replay past task data to alleviate forgetting. However, the overlapping data rather can cause *label conflict* as illustrated in Figure 3, which would not happen in realistic incremental scenarios. In the figure, the overlapping image contains both a person and a motorbike object. Consequently, this image is presented in both task  $t - 1$  and task  $t$  with different foreground labels while the remaining pixels are annotated as *background*. If the image, with motorbike pixels labeled accordingly and the person object marked as *background*, is saved in task  $t - 1$  and utilized in task  $t$ , the model encounters the same image twice with disparate labels: initially with the motorbike object identified as *motorbike* and the person as *background*, followed by the motorbike being labeled as *background* and the person as *person*. Since label conflict happens between the **same image**, this may worsen the confusion in distinguishing between previously learned classes (*motorbike*) and new ones (*person*).

### 3.4 PROPOSED SCENARIO: PARTITIONED

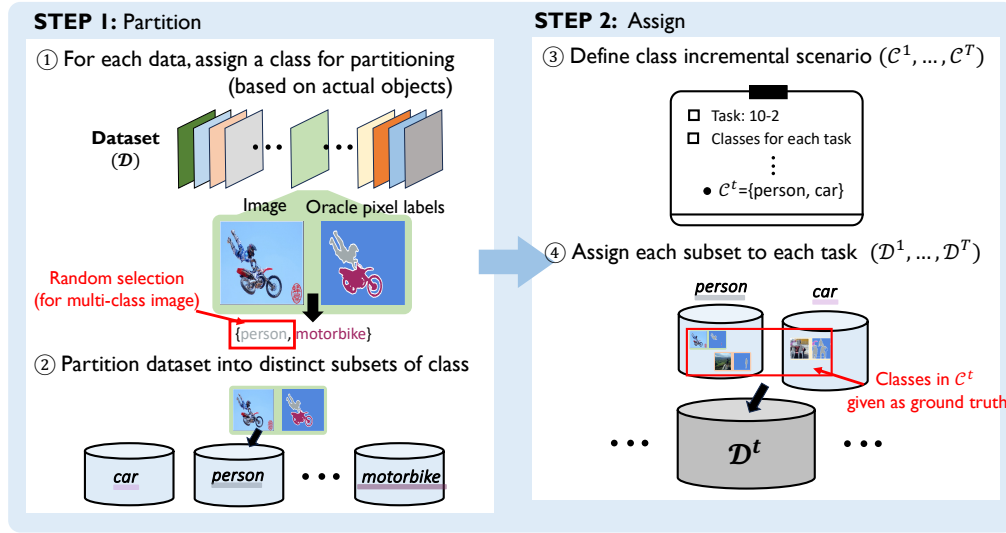
The issue of *overlapped* primarily arises from overlapping data that provide different labels in different tasks. Therefore, our proposed scenario aims to remove the existence of overlapping data by partitioning the whole dataset ( $\mathcal{D}$ ) into each task dataset ( $\mathcal{D}^0, \dots, \mathcal{D}^T$ ) in 2 steps: 1) partitioning the dataset into distinct subsets representing each class and 2) assigning each class subset to a corresponding task dataset.

Figure 4 demonstrates the process of constructing the proposed *partitioned* scenario. First, for each data (image-pixel labels pair), we assign a class for partitioning based on the oracle pixel labels. If the Oracle pixel labels consist of at least two classes, we randomly select one class. Robustness due to random selection is discussed in a later section. Second, we partition the whole dataset ( $\mathcal{D}$ ) into distinct subsets based on the assigned class for partitioning. Third, following the required task information (*e.g.*, task 10-2), we assign the ground truth classes for each incremental task ( $\mathcal{C}^0, \dots, \mathcal{C}^T$ ). Finally, we assign each subset to the corresponding task dataset ( $\mathcal{D}^0, \dots, \mathcal{D}^T$ ).

As summarized in Table 2, our proposed *partitioned* 1) guarantees disjointness between task datasets which eliminates overlapping data and 2) captures the background shift of both previous and unseen classes. Table 2 compares *parti-*

Table 2: Comparison of scenarios including *partitioned* in two criteria towards realistic CISS scenario.

	Removal of overlapping data	Capturing background shifts
disjoint	✓	✗
overlapped	✗	✓
partitioned (ours)	✓	✓

Figure 4: Illustration of dataset construction steps for *partitioned* scenario.

*tioned* with *disjoint* and *overlapped* in the context of two requirements towards the realistic scenario. Experimental results on *partitioned* with reproduced baselines and ablation studies on dataset construction are reported in Section 4.

### 3.5 NEW BASELINE FOR EXEMPLAR MEMORY REHEARSAL

From the experiments and analysis in Section 3.2, we contend that the problems of overlapping data were closely related to the retrieval of previous classes: one taking unwanted advantage of pseudo-labels and the other worsening label conflicts through data from exemplar memory. Since the issue of overlapping data is mitigated in our proposed scenario, it is natural to expect an effective usage of memory in *partitioned*. Therefore, we propose a simple yet competitive baseline that integrates MiB (Cermelli et al., 2020) with an extra loss function, tailored for the case of using exemplar memory.

Following notations in MiB (Cermelli et al., 2020), the overall loss function of our method at task  $t$  is defined as:

$$\mathcal{L}(\theta^t) = \underbrace{\frac{1}{|\mathcal{D}^t|} \sum_{(x,y) \in \mathcal{D}^t} \mathcal{L}_{uncke}(y, f_{\theta^t}(x)) + \frac{\lambda}{|\mathcal{D}^t \cup \mathcal{M}^{t-1}|} \sum_{(x,y) \in \mathcal{D}^t \cup \mathcal{M}^{t-1}} \mathcal{L}_{unkd}(f_{\theta^{t-1}}(x), f_{\theta^t}(x))}_{\text{From MiB (Cermelli et al., 2020)}} + \underbrace{\frac{1}{|\mathcal{M}^{t-1}|} \sum_{(x,y) \in \mathcal{M}^{t-1}} \mathcal{L}_{mem}(y, f_{\theta^t}^t(x))}_{\text{Our proposed memory loss}} \quad (4)$$

where  $\mathcal{L}_{uncke}(\cdot)$  and  $\mathcal{L}_{unkd}(\cdot)$  are the loss functions employed in MiB<sup>3</sup>. For the specific formulation of  $\mathcal{L}_{uncke}(\cdot)$  and  $\mathcal{L}_{unkd}(\cdot)$  in our notation, please refer to Section A.4. Regarding  $\mathcal{L}_{mem}(\cdot)$ , we suggest utilizing cross-entropy loss with the augmented predictions  $\hat{p}_{i,c}^t$  as follows:

$$\mathcal{L}_{mem}(y, f_{\theta^t}^t(x)) = -\frac{1}{|\mathcal{I}|} \sum_{i \in \mathcal{I}} \log \hat{p}_{i, y_i}^t. \quad (5)$$

Here,  $\hat{p}_{i, y_i}^t$  represents the augmented prediction probability (after softmax) for the ground truth label of a  $i^{th}$  pixel, i.e.,  $y_i$ . Moreover, the augmented prediction  $\hat{p}_{i,c}^t$  can be defined as follows:

$$\hat{p}_{i,c}^t = \begin{cases} p_{i,c}^t & \text{if } c \neq c_{bg} \\ p_{i,c_{bg}}^t + \sum_{k \in \mathcal{C}^t} p_{i,k}^t & \text{if } c = c_{bg}, \end{cases} \quad (6)$$

<sup>3</sup>The original paper utilizes the terminologies  $\mathcal{L}_{ce}(\cdot)$  and  $\mathcal{L}_{kd}(\cdot)$  to represent loss functions. However, to avoid potential confusion with conventional cross-entropy and knowledge distillation losses, we choose to adjust the terminology for the loss while maintaining the same format.

where  $p_{i,c}^t = \exp^{z_{i,c}^t} / \sum_{k \in \mathcal{C}^{0:t} \cup \{c_{bg}\}} \exp^{z_{i,k}^t}$  is the prediction probability (after softmax) for class  $c$  using  $f_{\theta^t}$ . Note that the softmax is calculated by normalizing the prediction scores (before softmax) of all the seen classes.

Note that the motivation behind employing Equation (5) stems from the background shift of data in  $\mathcal{M}^{t-1}$ . For example, consider a data stored in the exemplar memory containing objects belonging to the class of current task. Since data from  $\mathcal{M}^{t-1}$  has labels from  $\mathcal{C}^{0:t-1}$ , those objects are annotated as *background*. This induces a background shift problem of the current class and confuses the learning of the corresponding class in  $\mathcal{D}^t$ . To mitigate this conflict, we adopt the intuition of Zhang et al. (2022b), wherein both background and unseen classes are treated as the same class. Additionally, inspired by the prediction augmentation technique discussed in Cermelli et al. (2020), we aggregate the prediction values of  $c_{bg}$  and  $c \in \mathcal{C}^t$ , specifically in the case of  $c = c_{bg}$  in Equation (6). Note that this allows for a positive update of prediction scores for both background and new classes when the model is trained with pixels labeled as *background*, thereby alleviating the label conflict of the data in  $\mathcal{M}^{t-1}$ .

### 3.6 IMPLEMENTATION ISSUES IN PREVIOUS CISS STUDIES

In addition to the issues discussed in the previous sections, we will highlight a certain overlooked aspect of code implementation errors in CISS studies. It’s worth noting that the code implementation error of target labeling memory data is prevalent across recent studies (Cha et al., 2021; Baek et al., 2022; Zhang et al., 2022b; 2023). Upon examination of their official code repositories, it becomes evident that the data from the exemplar memory **do not provide ground truth** labels for previous objects; instead, they only assign *ground truth* labels based on  $\mathcal{C}^t$  or  $c_{bg}$  (refer to Figure 7 in the Appendix). We would like to emphasize the importance of accurate implementation as such discrepancy in implementation can lead to inherent experimental biases. To address this, we rectified the error in the implementation and conducted all experiments with the corrected version.

We believe that addressing these implementation corrections and providing reproduced baselines<sup>4</sup> constitutes a valuable contribution of our work, which can benefit future researchers in CISS studies.

## 4 EXPERIMENTAL RESULTS

### 4.1 EXPERIMENTAL SETUPS

**Dataset and protocols** We evaluated our methods based on two incremental scenarios, namely *overlapped* and *partitioned*, across several incremental tasks, such as 15-1 task, using Pascal VOC 2012 (Everingham et al., 2010) dataset. To assess the overall performance, we conducted evaluations across various tasks with differing characteristics, including large/small base tasks and varying numbers of incremental tasks. Note that the number of training data used for *overlapped* and *partitioned* scenarios differs, and detailed configurations are provided in the Appendix.

**Evaluation metrics** We utilize the mean Intersection-over-Union (mIoU) as our evaluation metric, which represents the averaged IoU for each class. The range of the average is provided in the table, distinguishing between base classes and incrementally learned classes. For instance, in the 15-1 task, classes 1 to 15 denote the base class list, while classes 16 to 20 indicate sequentially learned classes. Following Cermelli et al. (2020), the mIoU of the *background* class is only included in the *all* category, as it exists in both the base task and incremental tasks.

**Baseline** Since DKD (Baek et al., 2022) stands as one of the state-of-the-art methods in CISS and is implemented on Torch version, we reproduced the general regularization approaches, MiB (Cermelli et al., 2020) and PLOP (Douillard et al., 2021), based on its implementation. Note that pseudo-labeling is applied in MiB while DKD only relies on the ground truth labels of the foreground classes. The detailed implementation of memory usage, such as PLOP-M, DKD-M<sup>†</sup><sup>5</sup>, is explained in A.4. In this work, we assume the non-usage of the off-the-shelf detectors, thus we do not compare with the latest methods such as MicroSeg (Zhang et al., 2022b) and CoinSeg (Zhang et al., 2023).

**Implementation details** For all experiments, following Cermelli et al. (2020), we employed a DeepLab v3 segmentation network (Chen et al., 2017) with a ResNet-101 (He et al., 2016) backbone, pre-trained on ImageNet (Deng et al., 2009). For training our method (MiB-AugM), we optimize the network with the learning rate of  $10^{-3}$  for the backbone model and  $10^{-2}$  for the rest. SGD with a Nesterov momentum value of 0.9 is used for optimization in all incremental steps. Other training implementations are equal to details written in Cermelli et al. (2020). For detailed implementations of our model and other baselines, please refer to Section A.5. In terms of exemplar memory, consistent with prior research (Cha et al., 2021; Baek et al., 2022), we utilized memory with a fixed size of  $M = 100$ .

<sup>4</sup>Codes for all the baselines will be available in the camera-ready version

<sup>5</sup>Implementation of DKD with memory is modified from the original implementation, dubbed as DKD-M<sup>†</sup> as the original implementation, DKD-M, cannot be directly used after memory modification mentioned in Section 3.6



Table 3: Experimental results on Pascal VOC 2012

	15-1 Task						5-3 Task					
	overlapped			partitioned			overlapped			partitioned		
	1-15	16-20	all	1-15	16-20	all	1-5	6-20	all	1-5	6-20	all
MiB (Cermelli et al., 2020)	31.29	16.84	30.39	23.15	13.65	23.63	60.38	49.71	53.92	47.48	44.53	47.13
PLOP (Douillard et al., 2021)	63.94	12.86	50.98	62.69	8.31	46.76	23.53	32.01	32.52	16.59	28.23	28.04
PLOP-M (Douillard et al., 2021)	64.27	28.11	55.92	63.08	31.40	56.21	65.19	39.66	48.02	56.83	36.63	43.76
DKD (Baek et al., 2022)	76.08	39.60	67.93	69.57	32.50	61.63	64.07	51.07	55.93	60.96	47.32	52.52
DKD-M <sup>†</sup> (Baek et al., 2022)	<b>76.87</b>	<b>45.43</b>	<b>70.03</b>	<b>76.89</b>	<b>43.71</b>	<b>69.66</b>	<b>68.41</b>	53.73	58.91	65.87	52.19	57.21
MiB + AugM (Ours)	72.26	32.23	63.39	72.40	29.77	62.64	67.51	<b>59.63</b>	<b>62.82</b>	<b>67.66</b>	<b>60.05</b>	<b>63.17</b>
	10-1 Task						10-5 Task					
	overlapped			partitioned			overlapped			partitioned		
	1-10	11-20	all	1-10	11-20	all	1-10	11-20	all	1-10	11-20	all
MiB (Cermelli et al., 2020)	10.20	21.56	18.92	4.98	16.47	14.01	68.32	57.84	64.33	62.69	54.85	60.24
PLOP (Douillard et al., 2021)	25.61	11.23	17.55	11.81	8.95	9.89	59.27	50.93	56.78	49.99	45.94	50.00
PLOP-M (Douillard et al., 2021)	9.72	6.33	10.57	9.81	10.62	12.93	75.23	55.25	66.48	69.16	49.90	61.06
DKD (Baek et al., 2022)	71.77	45.68	59.94	67.03	43.79	56.87	71.70	57.97	66.06	69.69	54.88	63.64
DKD-M <sup>†</sup> (Baek et al., 2022)	<b>72.72</b>	<b>50.82</b>	<b>63.03</b>	<b>70.99</b>	<b>49.95</b>	<b>61.80</b>	72.49	56.92	65.95	70.36	55.51	64.27
MiB + AugM (Ours)	65.36	37.19	52.57	63.58	39.64	52.90	<b>74.83</b>	<b>61.75</b>	<b>69.32</b>	<b>72.51</b>	<b>59.19</b>	<b>67.00</b>

## 4.2 RESULTS

### 4.2.1 BASELINE RESULTS ON TWO SCENARIOS: OVERLAPPED AND PARTITIONED

**Memory efficiency in the overlapped scenario** Table 3 illustrates that all methods demonstrate a greater improvement in memory usage efficiency across every incremental task in the *partitioned* scenario compared to the *overlapped* scenario. For instance, figure 5b illustrates memory gains of each method at 5-3 task. The bottom bar and the dashed upper bar indicate mIoU without memory and the memory gain for each method, respectively. All the methods show a larger gain in *partitioned* compared to *overlapped*, and MiB shows the largest gain in *partitioned*. These results align with the previous assumption that the usage of memory was undermined in *overlapped* due to the label conflict and demonstrate that our proposed loss effectively mitigates forgetting.

**label conflicts in overlapped scenario** There are instances in both PLOP and DKD tasks where the utilization of memory adversely affects performance in *overlapped*, while gains are observed in *partitioned*. For instance, in the 10-1 task, PLOP demonstrates a decline from 17.55 to 10.57, while an increase of 3.04 is observed in *partitioned*. A similar phenomenon is observed in the 10-5 task for DKD. Note that this decline in *overlapped* may differ from results reported in the original papers, as previous studies consistently implemented memory labels incorrectly, as discussed in Section 3.6. These findings align with the second argument presented in Section 3.2, highlighting that overlapping data saved in memory can harm the model by worsening the label confusion.

**Robustness of partitioned scenario** Given that the data splitting rule used in *partitioned* entails randomness, we analyze the variance of methods trained on *partitioned* datasets constructed with different seeds. We also report the variance of models learned on *overlapped* that is not affected by the data order, which represents the default variance during training each method. The figures displayed above the bar plot in Figure 5c illustrate the performance variance of each method. Notably, the model trained on the *partitioned* dataset exhibits similar randomness to the default variance observed in the *overlapped* scenario. This suggests that the construction of the *partitioned* dataset is robust to variations in random seeds.

### 4.2.2 EXPERIMENTAL RESULTS ON MiB-AUGM

**MiB-AugM as a new baseline for plasticity** MiB with our proposed memory loss, MiB-AugM, exhibits state-of-the-art results across several incremental tasks. In Table 3, in both the *partitioned* 5-3 and 10-5 tasks, MiB-AugM outperforms the state-of-the-art method by 5.96 and 2.73, respectively. Additionally, Figure 5a demonstrates that this superiority remains consistent for every task.

While our proposed memory-based baseline may not demonstrate superior results in every task, we highlight two key points that support MiB-AugM as a promising future baseline for plasticity.

Firstly, MiB-AugM shows better performance in tasks that are more complex in terms of learning new concepts. As more classes are introduced in the new task, the model must distinguish not only between old and new classes but also among the new classes themselves. Hence, a higher level of plasticity is required, particularly in the 5-3 and

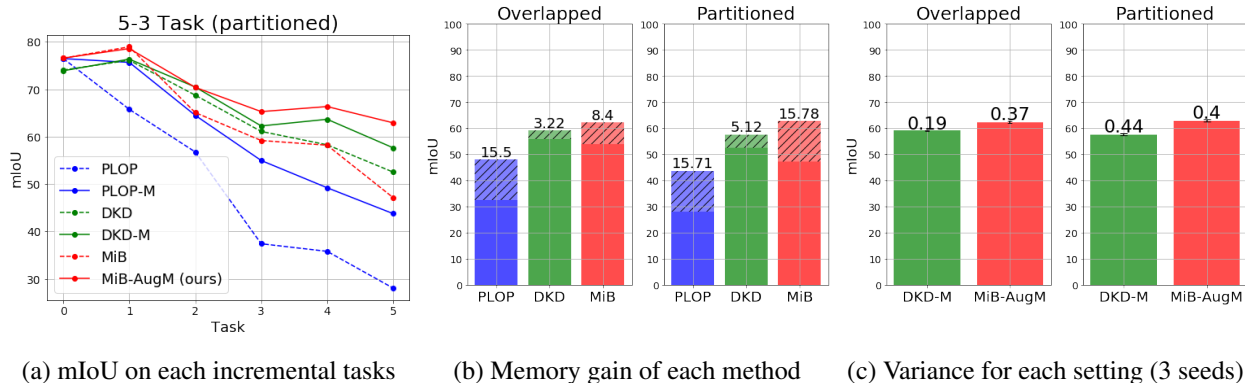


Figure 5: Results of each method on 5-3 Task

10-5 tasks. Secondly, MiB-AugM is an efficient method in terms of hyper-parameters. Unlike other methods that necessitate multiple hyper-parameters (at least 4 for DKD and PLOP), MiB-AugM has only  $\lambda$ .

Given that MiB-AugM can efficiently achieve state-of-the-art performance in several incremental tasks requiring complex plasticity, we insist that it holds promise as a valuable baseline for plasticity in future CISS studies.

## 5 CONCLUDING REMARKS

Our work tackles the unrealistic property of the overlapped setting in CISS. Namely, the identical images are reintroduced in future tasks with different pixel labels, which is far from a practical learning scenario. This assertion is reinforced by the observations that overlapping data may confer advantages or disadvantages to techniques widely used in CISS, thereby impacting algorithm development in practical applications. Therefore, we propose an alternative setting that eliminates the overlapping data while meeting the requirement of a realistic incremental scenario, such as capturing the background shift of previous and new classes. Additionally, we introduce a simple yet competitive exemplar memory-based method that addresses the background shifts occurring in the data stored in the exemplar memory. This method efficiently utilizes exemplar memory in the proposed setting and outperforms state-of-the-art methods on several tasks that learn multiple new classes at every incremental task. Furthermore, we are the first to identify and address code implementation issues related to exemplar memory retrieval, which is prevalent in CISS.

## 6 LIMITATIONS AND FUTURE WORK

While promising, our work has several limitations that warrant future exploration.

Firstly, our proposed replay-based baseline exhibits inferior performance compared to state-of-the-art methods in the 15-1 and 10-1 tasks, which involve learning a small number of classes in common. Addressing the stability-plasticity dilemma regarding the number of new classes requires further research.

Secondly, our findings are based on experiments conducted solely on the Pascal VOC dataset, which is relatively small. Future research should explore other datasets beyond Pascal VOC (Everingham et al., 2010) or ADE 20K (Zhou et al., 2017), with larger volumes of data. We intend to investigate incremental scenarios involving larger datasets as part of our future work.

## REFERENCES

- Hongjoon Ahn, Sungmin Cha, Donggyu Lee, and Taesup Moon. Uncertainty-based continual learning with adaptive regularization. *Advances in neural information processing systems*, 32, 2019.
- Hongjoon Ahn, Jihwan Kwak, Subin Lim, Hyeonsu Bang, Hyojun Kim, and Taesup Moon. Ss-il: Separated softmax for incremental learning. In *Proceedings of the IEEE/CVF International conference on computer vision*, pp. 844–853, 2021.
- Donghyeon Baek, Youngmin Oh, Sanghoon Lee, Junhyup Lee, and Bumsub Ham. Decomposed knowledge distillation for class-incremental semantic segmentation. *Advances in Neural Information Processing Systems*, 35: 10380–10392, 2022.
- Pietro Buzzega, Matteo Boschini, Angelo Porrello, Davide Abati, and Simone Calderara. Dark experience for general continual learning: a strong, simple baseline. *Advances in neural information processing systems*, 33:15920–15930, 2020.
- Gail A Carpenter and Stephen Grossberg. Art 2: Self-organization of stable category recognition codes for analog input patterns. *Applied Optics*, 26(23):4919–4930, 1987.
- Fabio Cermelli, Massimiliano Mancini, Samuel Rota Buló, Elisa Ricci, and Barbara Caputo. Modeling the background for incremental learning in semantic segmentation. In *Proceedings of the IEEE/CVF Conference on Computer Vision and Pattern Recognition*, pp. 9233–9242, 2020.
- Sungmin Cha, YoungJoon Yoo, Taesup Moon, et al. Ssul: Semantic segmentation with unknown label for exemplar-based class-incremental learning. *Advances in neural information processing systems*, 34:10919–10930, 2021.
- Arslan Chaudhry, Puneet K Dokania, Thalaiyasingam Ajanthan, and Philip HS Torr. Riemannian walk for incremental learning: Understanding forgetting and intransigence. In *Proceedings of the European conference on computer vision (ECCV)*, pp. 532–547, 2018.
- Jinpeng Chen, Runmin Cong, LUO Yuxuan, Horace Ip, and Sam Kwong. Saving 100x storage: Prototype replay for reconstructing training sample distribution in class-incremental semantic segmentation. In *Thirty-seventh Conference on Neural Information Processing Systems*, 2023.
- Liang-Chieh Chen, George Papandreou, Florian Schroff, and Hartwig Adam. Rethinking atrous convolution for semantic image segmentation. *arXiv preprint arXiv:1706.05587*, 2017.
- Aristotelis Chrysakis and Marie-Francine Moens. Online bias correction for task-free continual learning. *ICLR 2023 at OpenReview*, 2023.
- Jia Deng, Wei Dong, Richard Socher, Li-Jia Li, Kai Li, and Li Fei-Fei. Imagenet: A large-scale hierarchical image database. In *2009 IEEE conference on computer vision and pattern recognition*, pp. 248–255. Ieee, 2009.
- Arthur Douillard, Matthieu Cord, Charles Ollion, Thomas Robert, and Eduardo Valle. Podnet: Pooled outputs distillation for small-tasks incremental learning. In *Computer Vision—ECCV 2020: 16th European Conference, Glasgow, UK, August 23–28, 2020, Proceedings, Part XX 16*, pp. 86–102. Springer, 2020.
- Arthur Douillard, Yifu Chen, Arnaud Dapogny, and Matthieu Cord. Plop: Learning without forgetting for continual semantic segmentation. In *Proceedings of the IEEE/CVF conference on computer vision and pattern recognition*, pp. 4040–4050, 2021.
- Mark Everingham, Luc Van Gool, Christopher KI Williams, John Winn, and Andrew Zisserman. The pascal visual object classes (voc) challenge. *International journal of computer vision*, 88:303–338, 2010.
- Yasir Ghunaim, Adel Bibi, Kumail Alhamoud, Motasem Alfarra, Hasan Abed Al Kader Hammoud, Ameya Prabhu, Philip HS Torr, and Bernard Ghanem. Real-time evaluation in online continual learning: A new hope. In *Proceedings of the IEEE/CVF Conference on Computer Vision and Pattern Recognition*, pp. 11888–11897, 2023.
- Jiangpeng He, Runyu Mao, Zeman Shao, and Fengqing Zhu. Incremental learning in online scenario. In *Proceedings of the IEEE/CVF conference on computer vision and pattern recognition*, pp. 13926–13935, 2020.
- Kaiming He, Xiangyu Zhang, Shaoqing Ren, and Jian Sun. Deep residual learning for image recognition. In *Proceedings of the IEEE conference on computer vision and pattern recognition*, pp. 770–778, 2016.

- Geoffrey Hinton, Oriol Vinyals, and Jeff Dean. Distilling the knowledge in a neural network. *arXiv preprint arXiv:1503.02531*, 2015.
- Saihui Hou, Xinyu Pan, Chen Change Loy, Zilei Wang, and Dahua Lin. Learning a unified classifier incrementally via rebalancing. In *Proceedings of the IEEE/CVF conference on computer vision and pattern recognition*, pp. 831–839, 2019.
- Ching-Yi Hung, Cheng-Hao Tu, Cheng-En Wu, Chien-Hung Chen, Yi-Ming Chan, and Chu-Song Chen. Compacting, picking and growing for unforgetting continual learning. *Advances in Neural Information Processing Systems*, 32, 2019.
- Zhenchao Jin. Cssegmentation: An open source continual semantic segmentation toolbox based on pytorch. <https://github.com/SegmentationBLWX/cssegmentation>, 2023.
- Sangwon Jung, Hongjoon Ahn, Sungmin Cha, and Taesup Moon. Continual learning with node-importance based adaptive group sparse regularization. *Advances in neural information processing systems*, 33:3647–3658, 2020.
- James Kirkpatrick, Razvan Pascanu, Neil Rabinowitz, Joel Veness, Guillaume Desjardins, Andrei A Rusu, Kieran Milan, John Quan, Tiago Ramalho, Agnieszka Grabska-Barwinska, et al. Overcoming catastrophic forgetting in neural networks. *Proceedings of the national academy of sciences*, 114(13):3521–3526, 2017.
- Hyunseo Koh, Minhyuk Seo, Jihwan Bang, Hwanjun Song, Deokki Hong, Seulki Park, Jung-Woo Ha, and Jonghyun Choi. Online boundary-free continual learning by scheduled data prior. In *The Eleventh International Conference on Learning Representations*, 2022.
- Zhizhong Li and Derek Hoiem. Learning without forgetting. *IEEE transactions on pattern analysis and machine intelligence*, 40(12):2935–2947, 2017.
- Huiwei Lin, Baoquan Zhang, Shanshan Feng, Xutao Li, and Yunming Ye. Pcr: Proxy-based contrastive replay for online class-incremental continual learning. In *Proceedings of the IEEE/CVF Conference on Computer Vision and Pattern Recognition*, pp. 24246–24255, 2023.
- David Lopez-Paz and Marc’Aurelio Ranzato. Gradient episodic memory for continual learning. *Advances in neural information processing systems*, 30, 2017.
- Michael McCloskey and Neal J Cohen. Catastrophic interference in connectionist networks: The sequential learning problem. In *Psychology of learning and motivation*, volume 24, pp. 109–165. Elsevier, 1989.
- Martial Mermillod, Aurélie Bugaïska, and Patrick Bonin. The stability-plasticity dilemma: Investigating the continuum from catastrophic forgetting to age-limited learning effects. *Frontiers in Psychology*, 4:504, 2013.
- Umberto Michieli and Pietro Zanuttigh. Continual semantic segmentation via repulsion-attraction of sparse and disentangled latent representations. In *Proceedings of the IEEE/CVF conference on computer vision and pattern recognition*, pp. 1114–1124, 2021.
- Adam Paszke, Sam Gross, Soumith Chintala, Gregory Chanan, Edward Yang, Zachary DeVito, Zeming Lin, Alban Desmaison, Luca Antiga, and Adam Lerer. Automatic differentiation in pytorch. 2017.
- Ameya Prabhu, Philip HS Torr, and Puneet K Dokania. Gdumb: A simple approach that questions our progress in continual learning. In *Computer Vision—ECCV 2020: 16th European Conference, Glasgow, UK, August 23–28, 2020, Proceedings, Part II 16*, pp. 524–540. Springer, 2020.
- David Rolnick, Arun Ahuja, Jonathan Schwarz, Timothy Lillicrap, and Gregory Wayne. Experience replay for continual learning. *Advances in Neural Information Processing Systems*, 32, 2019.
- Andrei A Rusu, Neil C Rabinowitz, Guillaume Desjardins, Hubert Soyer, James Kirkpatrick, Koray Kavukcuoglu, Razvan Pascanu, and Raia Hadsell. Progressive neural networks. *arXiv preprint arXiv:1606.04671*, 2016.
- Hanul Shin, Jung Kwon Lee, Jaehong Kim, and Jiwon Kim. Continual learning with deep generative replay. *Advances in neural information processing systems*, 30, 2017.
- Xiaoyu Tao, Xiaopeng Hong, Xinyuan Chang, Songlin Dong, Xing Wei, and Yihong Gong. Few-shot class-incremental learning. In *Proceedings of the IEEE/CVF Conference on Computer Vision and Pattern Recognition*, pp. 12183–12192, 2020.

- Yue Wu, Yinpeng Chen, Lijuan Wang, Yuancheng Ye, Zicheng Liu, Yandong Guo, and Yun Fu. Large scale incremental learning. In *Proceedings of the IEEE/CVF conference on computer vision and pattern recognition*, pp. 374–382, 2019.
- Shipeng Yan, Jiangwei Xie, and Xuming He. Der: Dynamically expandable representation for class incremental learning. In *Proceedings of the IEEE/CVF conference on computer vision and pattern recognition*, pp. 3014–3023, 2021a.
- Shipeng Yan, Jiale Zhou, Jiangwei Xie, Songyang Zhang, and Xuming He. An em framework for online incremental learning of semantic segmentation. In *Proceedings of the 29th ACM international conference on multimedia*, pp. 3052–3060, 2021b.
- Yibo Yang, Haobo Yuan, Xiangtai Li, Zhouchen Lin, Philip Torr, and Dacheng Tao. Neural collapse inspired feature-classifier alignment for few-shot class incremental learning. *arXiv preprint arXiv:2302.03004*, 2023.
- Jaehong Yoon, Eunho Yang, Jeongtae Lee, and Sung Ju Hwang. Lifelong learning with dynamically expandable networks. *arXiv preprint arXiv:1708.01547*, 2017.
- Chang-Bin Zhang, Jia-Wen Xiao, Xialei Liu, Ying-Cong Chen, and Ming-Ming Cheng. Representation compensation networks for continual semantic segmentation. In *Proceedings of the IEEE/CVF Conference on Computer Vision and Pattern Recognition*, pp. 7053–7064, 2022a.
- Zekang Zhang, Guangyu Gao, Zhiyuan Fang, Jianbo Jiao, and Yunchao Wei. Mining unseen classes via regional objectness: A simple baseline for incremental segmentation. *Advances in Neural Information Processing Systems*, 35:24340–24353, 2022b.
- Zekang Zhang, Guangyu Gao, Jianbo Jiao, Chi Harold Liu, and Yunchao Wei. Coinseg: Contrast inter-and intra-class representations for incremental segmentation. In *Proceedings of the IEEE/CVF International Conference on Computer Vision*, pp. 843–853, 2023.
- Bolei Zhou, Hang Zhao, Xavier Puig, Sanja Fidler, Adela Barriuso, and Antonio Torralba. Scene parsing through ade20k dataset. In *Proceedings of the IEEE conference on computer vision and pattern recognition*, pp. 633–641, 2017.
- Lanyun Zhu, Tianrun Chen, Jianxiong Yin, Simon See, and Jun Liu. Continual semantic segmentation with automatic memory sample selection. In *Proceedings of the IEEE/CVF Conference on Computer Vision and Pattern Recognition*, pp. 3082–3092, 2023.

## A APPENDIX

## A.1 DATA CONFIGURATION COMPARISON: OVERLAP, DISJOINT, AND PARTITIONED

The tables in Table 4 provide a summary of the ground truth labels for each image in every incremental tasks. The first two columns show the image name and its corresponding oracle classes, while subsequent columns display the ground truth labels for each task. It’s important to note that pixels not belonging to classes in  $\mathcal{C}^t$  are annotated as the *background* class (abbreviated as *bg* in the table). To illustrate background shifts, pixels affected by unseen classes are highlighted in red, while those affected by previous classes are highlighted in blue. A hatched line is used for data not present in each task.

Table 4: Labeling information of each image in Figure 2 for each incremental scenario: *overlapped*, *Disjoint*, and *Ours*.

(a) Overlapped				(b) Disjoint				(c) Partitioned (Ours)						
Image	Oracle class	Given ground truth class			Image	Oracle class	Given ground truth class			Image	Oracle class	Given ground truth class		
		Task 1 (person)	Task 2 (motorbike)	Task 3 (car)			Task 1 (person)	Task 2 (motorbike)	Task 3 (car)			Task 1 (person)	Task 2 (motorbike)	Task 3 (car)
Img1	person	person	bg	bg	Img1	person	-	-	bg	Img1	person	-	bg	-
	motorbike	bg	motorbike	bg		motorbike	-	-	bg		motorbike	-	bg	-
	car	bg	bg	car		car	-	-	car		-	-	-	
Img2	person	person	bg	-	Img2	person	-	bg	-	Img2	person	-	bg	-
	motorbike	bg	motorbike	-		motorbike	-	motorbike	-		motorbike	-	motorbike	-
Img3	car	-	-	car	Img3	car	-	-	car	Img3	car	-	-	car
Img4	person	person	-	bg	Img4	person	-	-	bg	Img4	person	person	-	-
	car	bg	-	car		car	-	-	car		car	bg	-	-
Img5	person	person	-	-	Img5	person	person	-	-	Img5	person	person	-	-

Similar to data configuration in CIL, the *disjoint* scenario in CISS ensures the separation of data from each task. However, achieving disjointness in the *disjoint* scenario requires prior knowledge of unseen classes and excludes data that could cause background shifts of these unseen classes (indicated by the absence of *bg* in the table). Given that background shift poses a significant challenge in CISS, many studies opt for the *overlapped* scenario, which can result in background shifts of both previous and unseen classes. However, in this work, we highlight the issues associated with overlapping data in the *overlapped* scenario and propose a novel scenario called *partitioned*. Our proposed scenario ensures the separation between task data while accommodating background shifts of both unseen and previous classes.

Table 5: The number of train data for every task in the *overlapped* and *partitioned* scenarios.

Task	Scenario	Seed	The number of training data for each task	Total
15-1 Task	overlapped	-	9568 / 487 / 299 / 491 / 500 / 548	11893
		0	9031 / 254 / 266 / 270 / 434 / 327	10582
	partitioned	1	9059 / 263 / 271 / 256 / 413 / 320	10528
		2	9030 / 274 / 258 / 253 / 437 / 330	10582
5-3 Task	overlapped	-	2836 / 2331 / 1542 / 2095 / 4484 / 1468	14756
		0	2222 / 1860 / 972 / 1574 / 2923 / 1031	10582
	partitioned	1	2237 / 1859 / 991 / 1616 / 2890 / 989	10582
		2	2221 / 1855 / 993 / 1589 / 2904 / 1020	10582
10-1 Task	overlapped	-	6139 / 528 / 1177 / 444 / 482 / 3898 / 487 / 299 / 491 / 500 / 548	14993
	partitioned	0	4847 / 207 / 961 / 310 / 303 / 2403 / 254 / 266 / 270 / 434 / 327	10582
10-5 Task	overlapped	-	6139 / 5542 / 2145	13826
	partitioned	0	4847 / 4148 / 1551	10582

Table 5 demonstrates the number of data  $\mathcal{D}^t$  used for each task in both the *partitioned* and *overlapped* scenarios. Note that the dataset remains consistent across tasks in the *overlapped*, whereas variations are observed in the *partitioned* scenario across different seeds.

## A.2 PSEUDO RETRIEVAL RATE (PRR)

## A.2.1 OVERVIEW

Figure 6 illustrates the pseudo retrieval rate (PRR) metric. In the figure,  $\mathcal{D}_p^t$  represents a subset of  $\mathcal{D}^t$  specific to the *partitioned* protocol, containing data points with both new and old object classes. We evaluate the PRR metric using the model trained up to the previous task, denoted as  $f_{\theta^{t-1}}(\cdot)$ .

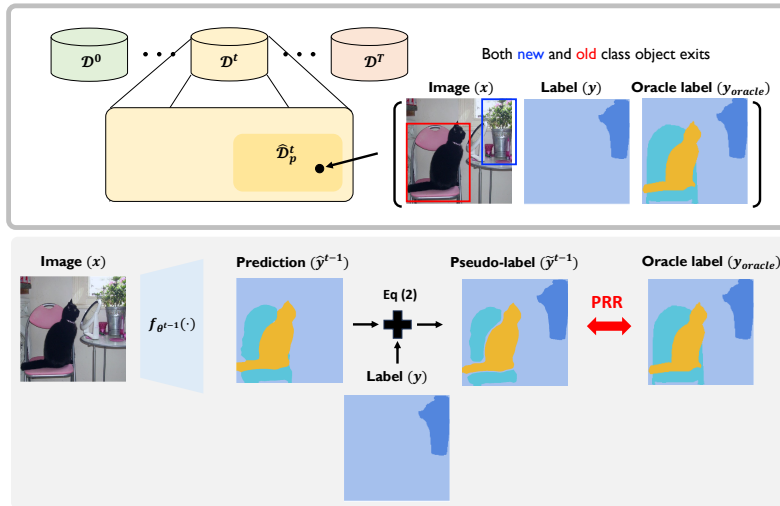


Figure 6: An overview of  $\hat{\mathcal{D}}_p^t$  and Pseudo-labeling Retrieval Rate (PRR) metric

## A.3 IMPLEMENTATION ERROR IN PREVIOUS STUDIES

As illustrated in Figure 7, the model is expected to see ground-truth masks annotated with *motorbike* class for current data and *person* class for data stored in memory, respectively. However, following code implementation of previous studies (Cha et al., 2021; Baek et al., 2022; Zhang et al., 2022b; 2023), the ground-truth mask for memory data is labeled with *motorbike* class.

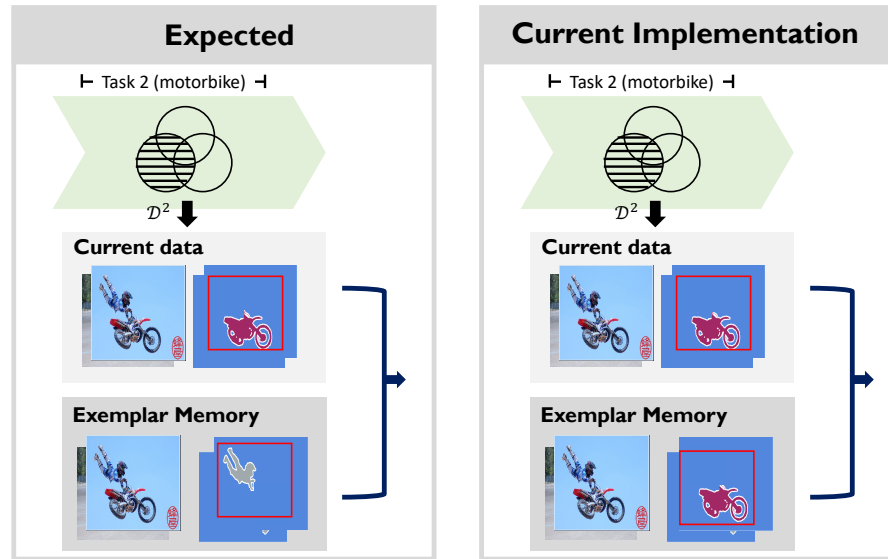


Figure 7: This figure illustrates the labeling issue in code implementation of current CISS studies (Cha et al., 2021; Baek et al., 2022; Zhang et al., 2022b; 2023). Note that the ground-truth mask of data from the exemplar memory does not provide labels for the classes of the previous task at which it was stored. Instead, it provides labels for the classes of the current task.



#### A.4 IMPLEMENTATION OF MiB-AUGM, PLOP-M, AND DKD-M<sup>†</sup>

In this section, we explain the concrete formula of MiB-AugM, PLOP-M, and DKD-M<sup>†</sup> following the notation in Section 3.1.

##### A.4.1 MiB-AUGM

The overall loss for MiB-AugM model can be defined as follows.

$$\mathcal{L}(\theta^t) = \underbrace{\frac{1}{|\mathcal{D}^t|} \sum_{(x,y) \in \mathcal{D}^t} \mathcal{L}_{uncke}(y, f_{\theta^t}(x)) + \frac{\lambda}{|\mathcal{D}^t \cup \mathcal{M}^{t-1}|} \sum_{(x,y) \in \mathcal{D}^t \cup \mathcal{M}^{t-1}} \mathcal{L}_{unkd}(f_{\theta^{t-1}}(x), f_{\theta^t}(x))}_{\text{From MiB (Cermelli et al., 2020)}} + \underbrace{\frac{1}{|\mathcal{M}^{t-1}|} \sum_{(x,y) \in \mathcal{M}^{t-1}} \mathcal{L}_{mem}(y, f_{\theta^t}(x))}_{\text{Our proposed memory loss}} \quad (7)$$

Here, we rewrite the formula of  $\mathcal{L}_{uncke}$  and  $\mathcal{L}_{unkd}$  defined in Cermelli et al. (2020) on our notation.

$$\mathcal{L}_{uncke}(y, f_{\theta^t}(x)) = -\frac{1}{|\mathcal{I}|} \sum_{i \in \mathcal{I}} \log \ddot{p}_{i,y_i}^t \quad (8)$$

$$\mathcal{L}_{unkd}(f_{\theta^{t-1}}(x), f_{\theta^t}(x)) = -\frac{1}{|\mathcal{I}|} \sum_{i \in \mathcal{I}} \sum_{c \in \mathcal{C}^{0:t-1}} p_{i,c}^{t-1} \log \dot{p}_{i,c}^t \quad (9)$$

where  $\dot{p}_{i,c}^t$  and  $\ddot{p}_{i,c}^t$  indicates different augmentation technique of prediction probabilities. The augmented prediction for  $\mathcal{L}_{uncke}$ ,  $\ddot{p}_{i,c}^t$ , is defined as follows.

$$\ddot{p}_{i,c}^t = \begin{cases} p_{i,c}^t & \text{if } c \neq c_{bg} \\ p_{i,c_{bg}}^t + \sum_{k \in \mathcal{C}^{0:t-1}} p_{i,k}^t & \text{if } c = c_{bg} \end{cases} \quad (10)$$

##### A.4.2 PLOP-M

The loss function in PLOP-M remains unchanged, same as PLOP (Douillard et al., 2021). However, PLOP-M distinguishes itself by updating with concatenated data from both the current task and memory, using an equal ratio from each.

$$\mathcal{L}(\theta^t) = \frac{1}{|\mathcal{D}^t \cup \mathcal{M}^{t-1}|} \sum_{(x,y) \in \mathcal{D}^t \cup \mathcal{M}^{t-1}} \mathcal{L}_{ce}(\tilde{y}, f_{\theta^t}(x)) + \lambda \mathcal{L}_{pod}(f_{\theta^{t-1}}(x), f_{\theta^t}(x)) \quad (11)$$

##### A.4.3 DKD-M<sup>†</sup>

The loss function in DKD-M in the original paper remains also unchanged in its original paper (Baek et al., 2022). Namely, the data from concatenated set, *i.e.*,  $(x, y) \sim \mathcal{D}^t \cup \mathcal{M}^{t-1}$ , was forwarded to  $\mathcal{L}_{kd}$ ,  $\mathcal{L}_{dkd}$ ,  $\mathcal{L}_{mbce}$ , and  $\mathcal{L}_{ac}$ . However, looking at  $\mathcal{L}_{mbce}$  in eq 13, it only updates the new class score, which is awkward for data in memory that does not have any labels of new classes.

$$\mathcal{L}_{mbce}(y, f_{\theta^t}(x)) = -\frac{1}{|\mathcal{I}|} \sum_{i \in \mathcal{I}} \sum_{c \in \mathcal{C}^t} \gamma \mathbf{1}_{\{y_i=c\}} \log p_{i,c}^t + \mathbf{1}_{\{y_i \neq c\}} \log(1 - p_{i,c}^t) \quad (12)$$

Later, we noticed that this wrong usage did not harm the performance because the labeling issue existed in memory retrieval mentioned in Section 3.6 (Manuscript). Therefore, after correction in memory target labeling, we add a  $\mathcal{L}_{mbce}$  loss for memory, dubbed as  $\mathcal{L}_{membce}$ , which is defined as follows.

$$\mathcal{L}_{mbce}(y, f_{\theta^t}(x)) = -\frac{1}{|\mathcal{I}|} \sum_{i \in \mathcal{I}} \sum_{c \in \mathcal{C}^{0:t-1}} \gamma \mathbf{1}_{\{y_i=c\}} \log p_{i,c}^t + \mathbf{1}_{\{y_i \neq c\}} \log(1 - p_{i,c}^t) \quad (13)$$

The overall loss function for DKD-M<sup>†</sup> is as follows.

$$\begin{aligned} \mathcal{L}(\theta^t) = & \frac{1}{|\mathcal{D}^t \cup \mathcal{M}^{t-1}|} \sum_{(x,y) \in \mathcal{D}^t \cup \mathcal{M}^{t-1}} \underbrace{\left[ \alpha \mathcal{L}_{kd}(f_{\theta^{t-1}}(x), f_{\theta^t}(x)) + \beta \mathcal{L}_{dkd}(f_{\theta^{t-1}}(x), f_{\theta^t}(x)) \right]}_{\text{From DKD (Baek et al., 2022)}} \\ & + \frac{1}{|\mathcal{D}^t|} \sum_{(x,y) \in \mathcal{D}^t} \underbrace{\left[ \mathcal{L}_{mbce}(y, f_{\theta^t}(x)) + \mathcal{L}_{ac}(y, f_{\theta^t}(x)) \right]}_{\text{From DKD (Baek et al., 2022)}} \\ & + \frac{1}{|\mathcal{M}^{t-1}|} \sum_{(x,y) \in \mathcal{M}^{t-1}} \underbrace{\mathcal{L}_{mbce}(y, f_{\theta^t}(x))}_{\text{Added loss modified from } \mathcal{L}_{mbce}} \end{aligned} \quad (14)$$

## A.5 IMPLEMENTATION DETAILS

**Baseline reproduction and experimental environment** The code environment of CISS is divided into two branches: Distributed data parallel (DDP) implemented on Nvidia Apex (<https://github.com/NVIDIA/apex>) and Torch (Paszke et al., 2017). Initial studies primarily utilized the former, with Jin (2023) organizing numerous baselines for evaluation. Due to the transition of Nvidia Apex to Torch in deep learning community<sup>6</sup>, recent CISS works began to work on Torch environment. However, recent works conducted on the latter omitted the process of re-implementing baselines, instead reporting figures from the original paper. Given the transition from Apex to Torch, resulting in significant changes in built-in operations, it’s widely acknowledged that a mismatch in results exists between the two environments. To facilitate fair comparisons, we report our implementation of two baselines in the Torch version.

**Dataset and protocols** Pascal VOC 2012 (Everingham et al., 2010) consists of 10,582 training and 1,449 validation images for 20 object and background classes. For the training image, random crop with size 512, random resize with (0.5, 2.0) ratio, and normalization are used. For the test image, only normalization is used.

Following Cermelli et al. (2020), incremental tasks are denoted by the number of classes used in base classes,  $|C^0|$ , and the number of classes learned in each incremental task,  $|C^t| \forall t \in \{1, \dots, T\}$ . For example, if the base task class is composed of 15 classes and 1 class is learned at every task, it is denoted as 15-1 task.

**Training details** Table 6 summarizes the training details used for each method. MiB, PLOP-M, and DKD-M use the same details as MiB-AugM, PLOP, and DKD, respectively. Note that some training details of MiB are different from those that were used in MiB.

Table 6: Training details for each method

	Common					Base task		Incremental task	
	Batch size	Epoch	Optimizer	Momentum	Lr schedule	Lr (backbone / aspp / classifier)	Weight decay	Lr (backbone / aspp / classifier)	Weight decay (backbone / aspp / classifier)
PLOP (Douillard et al., 2021)	24	30	SGD	Nesterov, 0.9	PolyLR	0.01 / 0.01 / 0.01	0.001	0.001 / 0.001 / 0.001	0.001 / 0.001 / 0.001
DKD (Baek et al., 2022)	32	60	SGD	Nesterov, 0.9	PolyLR	0.001 / 0.01 / 0.01	0.0001	0.0001 / 0.001 / 0.001	0 / 0 / 0.0001
MiB-AugM (Ours)	24	30	SGD	Nesterov, 0.9	PolyLR	0.01 / 0.01 / 0.01	0.001	0.001 / 0.01 / 0.01	0 / 0 / 0.001

## A.5.1 HYPER-PARAMETERS

Table 7 summarizes the main hyper-parameters of each method used for training. Notations for each hyper-parameter are from the original paper. We also used same hyper-parameter used in MiB (Cermelli et al., 2020).

Table 7: Hyper-parameters used for each method

	Base task training	Incremental task	Inference
PLOP (Douillard et al., 2021)	-	$\lambda_f = 0.01$ (features), $\lambda_l = 0.0005$ (logits), $\tau = 0.001$ , pod scale= $[1, \frac{1}{2}, \frac{1}{4}]$	-
DKD (Baek et al., 2022)	$\gamma = 2$	$\alpha = 5, \beta = 5, \gamma = 1$	$\tau = 0.5$
MiB-AugM (Ours)	-	$\lambda = 5$	-

<sup>6</sup>Please refer to <https://github.com/NVIDIA/apex/issues/818>

## A.6 COMPUTATION DETAILS

The experiments were conducted using PyTorch (Paszke et al., 2017) 1.13.1 with CUDA 11.2 and were run on four NVIDIA Titan XP GPUs with 12GB memory per device. All experiments except PLOP (Douillard et al., 2021) were conducted with distributed data-parallel training on four GPUs. For PLOP (Douillard et al., 2021) experiments, we use 2 GPUs for parallel training since the results of the original paper could not be achieved by other numbers.

## A.7 SOFTWARE AND DATASET LICENSES

### A.7.1 DATASETS

- Pascal VOC (Everingham et al., 2010): CC BY-NC-SA 3.0 License  
<http://host.robots.ox.ac.uk/pascal/VOC/>

### A.7.2 MODELS

- MiB (Cermelli et al., 2020): MiT License  
<https://github.com/fcd194/MiB>
- PLOP (Douillard et al., 2021): MiT License  
[https://github.com/arthurdouillard/CVPR2021\\_PLOP](https://github.com/arthurdouillard/CVPR2021_PLOP)
- DKD (Baek et al., 2022): GPL-3.0 License  
<https://github.com/cvlab-yonsei/DKD>